

PACS numbers: 87.15.Vv; 87.64.Aa; 87.64.Cc
DOI: 10.1070/QE2006v036n12ABEH013331

Application of backward diffuse reflection spectroscopy for monitoring the state of tissues in photodynamic therapy

A.A. Stratonnikov, G.A. Meerovich, A.V. Ryabova, T.A. Savel'eva, V.B. Loshchenov

***Abstract*. The application of backward diffuse reflection (BDR) spectroscopy for *in vivo* monitoring the degree of haemoglobin oxygenation and concentration of photosensitisers in tissues subjected to photodynamic therapy is demonstrated. A simple experimental technique is proposed for measuring diffuse reflection spectra. The measurements are made under steady-state conditions using a fibreoptic probe with one transmitting and one receiving fibre separated by a fixed distance. Although this approach does not ensure the separation of contributions of scattering and absorption to the spectra being measured, it can be used for estimating the degree of haemoglobin oxygenation and concentration of photosensitisers in the tissues. Simple expressions for estimating the concentration of photosensitisers from the BDR spectra are presented and the accuracy of this approach is analysed. The results of application of BDR spectroscopy for monitoring various photosensitisers are considered.**

Keywords: *optical diagnostics, diffuse reflection spectroscopy, multiple scattering, photodynamic therapy, photosensitisers.*

1. Introduction

Backward diffuse reflection (BDR) spectroscopy is widely used for diagnostics and monitoring of various physiological processes in tissues. During the last three decades following the pioneering publication by Jöbsis [1], where the application of BDR spectroscopy in the IR range for noninvasive monitoring of haemoglobin oxygenation was demonstrated, this technique was improved and the range of its application was considerably broadened (see review [2] and references therein). At present, BDR spectroscopy is employed, in addition to monitoring oxygenation of haemoglobin and respiratory chain enzymes (cytochromes), in diagnostics of cancer of skin [3], urinary bladder [4], rectum [5], gastrointestinal tract [6], in gynaecology [7], and for diagnostics of cancer in other parts of the body. This technique has also found broad applications in monitoring exogenous photosensitisers (PSs) used in photodynamic therapy (PDT) [8 – 14], as well as various chemotherapy agents [15]. When BDR spectroscopy is used in cancer diagnostics, researchers usually try to find typical features directly in the spectra, which are different for tumours and normal tissues (tumour signature). When the same technique is used for monitoring oxygenation and exogenous PSs, it is necessary to separate the contribution of absorption in pure form and then to determine the concentration of chromophores in tissues by analysing the wavelength dependence of the absorption coefficient, as is usually done in the absorption spectroscopy of nonscattering media.

To separate the contributions from absorption and scattering to the diffuse reflection spectrum, time-resolved methods should be used [11, 16] or diffuse reflection should be measured simultaneously for several distances between the transmitting and receiving fibres [12, 13, 17]. Both approaches, especially the first one, require the use of a complex and expensive equipment and cumbersome analysis of experimental data; this complicates the application of these approaches in routine everyday tests. The use of the second technique, in which the receiving fibre is scanned relative to the transmitting fibre substantially prolongs the measuring time and is inconvenient for *in vivo* measurements. Here, we describe a simple method, in which the BDR spectra are measured in the stationary regime at the same fixed distance between the transmitting and receiving fibres. Such an approach is used in PDT both for monitoring the degree of haemoglobin oxygenation and for estimating the PS concentration in tissues (the PS concentration in tissues is measured by the standard sample technique).

2. *In vivo* backward diffuse reflection spectroscopy

The experimental setup for *in vivo* measurements of the BDR spectra is shown in Fig. 1. Light from halogen lamp (*1*) in a spectral range of 400 – 1100 nm was focused to the end of transmitting optical fibre (*2*). Transmitting fibres were silica single fibres of diameter 600 – 1000 μm with the numerical aperture NA = 0.22 or glass fibre bundles 3 – 5 mm in diameter with the numerical aperture NA = 0.45. We used bundles in the case of large distances between the transmitting and receiving fibres, when a high incident radiation power (up to 100 mW) was required. The transmitting fibre delivered light to tissue (*3*). The light passed through the tissue [see inset (*7*) in Fig. 1], where it experienced scattering and absorption, and was coupled to

A.A. Stratonnikov, G.A. Meerovich, A.V. Ryabova, T.A. Savel'eva, V.B. Loshchenov Natural Science Center, A.M. Prokhorov General Physics Institute, Russian Academy of Sciences, ul. Vavilova 38, 119991 Moscow, Russia; e-mail: alstrat77@mail.ru

Received 7 July 2006; revision received 7 August 2006
Kvantovaya Elektronika **36** (12) 1103 – 1110 (2006)
Translated by Ram Wadhwa

receiving fibre (*4*). As the latter we used silica single fibres 200 μm in diameter or fibre bundles consisting of seven such fibres, which were hexagonally packed on the side of the tissue to ensure spatial localisation of detection of light on the surface of the tissue; on the side of the spectrometer, the fibres were packed in a line to preserve the spectral resolution. Such a structure of the bundle provided the sevenfold increase in the intensity of light scattered in the tissue and collected on a detector, by preserving the required spectral resolution.

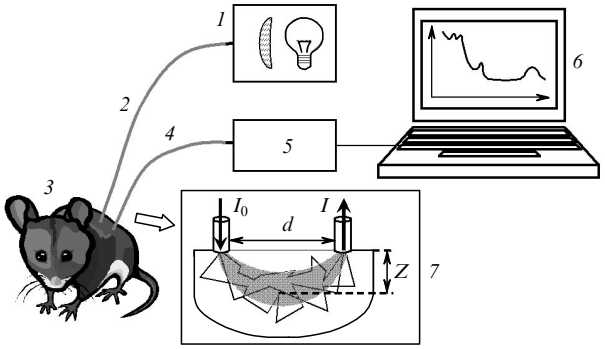

Figure 1. Scheme of the experimental setup for *in vivo* measuring BDR spectra of tissues: (*1*) halogen lamp; (*2*) transmitting fibre; (*3*) tissue under study; (*4*) receiving fibre; (*5*) spectrometer; (*6*) PC. Inset (*7*) shows scattering and absorption of light in the tissue.

The receiving and transmitting fibres were usually in direct contact with the tissue being tested or at a small distance (up to 1 mm) from its surface to avoid the effect of pressing on its optical properties. Because the distance d between the fibres was greater than 3 mm, the Fresnel reflection from the tissue was not recorded. Light from the receiving fibre was directed to spectrometer (*5*), which was controlled by PC (*6*) through an USB interface with the help of specially developed software. The spectrometer was a LESA-5 fibreoptic spectrometer (Biospec Ltd). The spectral sensitivity of the detector, the transmission spectrum of the fibres, and the emission spectrum of the light source were taken into account by performing measurements relative to the standard $BaSO_4$ sample with the reflection coefficient close to unity in the spectral range under study. The obtained results are usually presented in the form of the spectral dependence of the reflection coefficient $R(\lambda) = I/I_0$, or the logarithm of its reciprocal $A = \ln(1/R)$. Because the value of A also depends on the scattering coefficient of the tissue, we shall call it attenuation. The quantities I and I_0 are the measured values of the signals reflected from the tissue and the standard $BaSO_4$ sample, respectively. Because the wavelength dependence of I_0 can be measured within a certain constant factor, the reflection coefficient $R(\lambda)$ is also measured within a certain constant factor and the attenuation $A(\lambda)$ is determined within a certain additive constant, which is independent of the wavelength. The value of this constant is insignificant for our analysis of experimental data.

Note that, speaking of the diffuse reflection coefficient, a different geometry of measurements is usually implied, in which light diffusely reflected from the tissue is collected in close proximity of the illuminated region with the help of either an integrating sphere or a receiving fibre located at a certain distance from the tissue surface, so that the light collection aperture covers the entire area of the tissue from which diffusely reflected light emerges. In this case, the major part of collected photons propagate over a relatively short path in the tissue of the order of a few light penetration depths in the tissue (the penetration depth for skin is 1–2 mm in the visible and near-IR ranges). The reflection coefficient measured in this way will be henceforth referred to as the local reflectance. In this measuring geometry, photons incident on the detector have propagated both over short and long paths. If optical fibres spaced by a certain distance d from one another are used for collecting light, the photon mean path $\langle L \rangle$ in the tissue and the probe depth Z can be varied by changing this distance [see inset (*7*) in Fig. 1].

The diffuse reflectance R depends first of all on the absorption coefficient and the reduced scattering coefficient, as well as on the spatial distribution of these coefficients in tissue (layered structure of the tissue [18], pigment 'packing' effect [19–21], etc.). The layered structure of the tissue plays an important role in the local measurement of the reflectance because a part of light may experience diffuse reflection before reaching deeper layers where blood vessels are located. The contribution of the upper tissue layers (in particular, epidermis, in which capillaries and, hence, haemoglobin are absent) to the value of the reflectance measured using the scheme with separated fibres can be estimated by comparing the relative path lengths of photons in the epidermis and in deeper layers of the tissue. In the given measuring geometry, the photon path on the trajectory between the transmitting and receiving fibre in deeper layers of the tissue is two orders of magnitude longer than in the epidermis.

The diffuse reflectance for a spatially homogeneous medium can be represented by the integral

$$R = \frac{I}{I_0} = \int_0^\infty P(\mu_s', l) \exp(-\mu_a l) \mathrm{d}l, \qquad (1)$$

where μ_a and μ_s' are the absorption coefficient and reduced scattering coefficient; l is the photon path length in the tissue; and P is the photon path length distribution function. The dimensionless quantity $P(\mu_s', l)\mathrm{d}l$ is the probability that the photon path in the tissue between the transmitting and receiving fibres lies in the interval $[l, l + \mathrm{d}l]$. The photon path distribution function is determined by the experimental geometry (distance d between the fibres, their numerical aperture, the distance between the fibres and the tissue surface, etc.) and depends on the scattering properties of the medium (reduced scattering coefficient μ_s'). Generally speaking, we should take into account the dependence of P on the scattering coefficient μ_s and on the scattering anisotropy factor g, which are related to the reduced scattering coefficient by the expression $\mu_s' = \mu_s(1 - g)$. However, we will assume for simplicity that the value of P is determined by quantity μ_s'.

It is obvious that the photon path distribution function when measuring absorption spectra in a nonscattering medium with the photon path L, is the Dirac delta-function $P(l) = \delta(l - L)$. Substitution of this function into expression (1) naturally leads to the Lambert–Beer law describing the attenuation of light in an absorbing nonscattering medium:

$$\frac{I}{I_0} = \int_0^\infty \delta(l - L)\exp(-\mu_a l)\mathrm{d}l = \exp(-\mu_a L). \quad (2)$$

In the presence of scattering, the trajectories of photons incident on the detector have different lengths, which leads to blurring of the distribution function P. Exact analytic expressions for the path distribution function and for the reflectance do not exist even for the simplest geometry of a semi-infinite homogeneous medium; however, various approximate approaches to solving this problem exist. One of the approaches, which is called the modified Lambert – Beer law, is used for analysing the variations in the diffuse reflection spectra caused by relatively small variations in the absorption coefficient of the medium,

$$A = \ln R^{-1} = A_0 + \langle L\rangle\mu_a, \quad (3)$$

where A_0 is the attenuation of the signal in the medium in the absence of absorption and $\langle L\rangle$ is the photon path in the tissue, which is averaged in a certain manner. Depending on the definition of quantity $\langle L\rangle$, the modified Lambert – Beer law in form (3) can generally correspond to completely different approaches describing various approximations. Generally, $\langle L\rangle$ stands for the photon mean path in the tissue, which is expressed in terms of the photon path distribution function:

$$\langle L\rangle = \frac{\partial A}{\partial \mu_a} = \int_0^\infty lP(l)\exp(-\mu_a l)\mathrm{d}l \Big/ \int_0^\infty P(l)\exp(-\mu_a l)\mathrm{d}l. \quad (4)$$

However, in such a representation of $\langle L\rangle$, the modified Lambert – Beer law is valid only for small variations of μ_a. In the general case, when variations of μ_a are large, expression (3) holds if the following expression for $\langle L\rangle$ is used [22]:

$$\langle L\rangle_{\mathrm{int}} = \frac{1}{\mu_a}\int_0^{\mu_a}\langle L\rangle\mu_a^*\mathrm{d}\mu_a^* = \frac{1}{\mu_a} \times \int_0^{\mu_a}\left[\int_0^\infty lP(l)\exp(-\mu_a^* l)\mathrm{d}l \Big/ \int_0^\infty P(l)\exp(-\mu_a^* l)\mathrm{d}l\right]\mathrm{d}\mu_a^*. \quad (5)$$

Unlike expression (4), the integrated mean value of the photon path in the interval between 0 and μ_a is used here. The modified Lambert – Beer law using expression (5) for the mean path is valid in the general case. This can be easily verified: by substituting expression (5) into (3) and differentiating both sides of the resultant equation with respect to μ_a, we obtain an exact identity. From the point of view of practical application, however, expression (5) or even formula (4) for the photon mean path does not contribute much towards an interpretion of the diffuse reflection spectra on the basis of the modified Lambert – Beer law because the quantity $\langle L\rangle$ itself in this case is a complicated function of μ_a and μ_s'. For practical applications of this law, it is necessary to approximate the photon mean path by a simpler expression.

For analysing diffuse reflection spectra in the case of small variations of μ_a and μ_s', we can write the modified Lambert – Beer law in the differential form

$$\Delta A = \langle L\rangle|_{\mu_a=\mu_a^0}\Delta\mu_a, \quad \mu_a = \mu_a^0 + \Delta\mu_a, \quad (6)$$

where μ_a^0 is the absorption coefficient of the tissue in the absence of PSs and $\langle L\rangle$ is defined by formula (4). Note that the value of $\langle L\rangle$ defined in this way is independent of $\Delta\mu_a$; in the case when variations of μ_s' in the spectral range under investigation are also small, we can approximately assume that the value of $\langle L\rangle$ is also independent of the wavelength. Although expression (6) is substantiated only for small variations of μ_a, this approximation can be also used beyond its formal range of application, as is often the case. The applicability of this approximation for relatively large variations of the absorption coefficient was considered in detail in [23], where it was demonstrated that the modified Lambert – Beer law can be used for $\Delta\mu_a \sim \mu_a^0$ also.

Another approach that can be employed for interpreting the reflection spectra is the diffusion approximation. In this approximation, the photon path distribution function for a semi-infinite homogeneous medium with transmitting and receiving fibres separated by a distance d is defined as [24]

$$P(l) = z_0(4\pi D)^{-3/2}l^{-5/2}\exp\left(-\frac{d^2 + z_0^2}{4Dl}\right), \quad (7)$$

where $z_0 = 1/\mu_s'$ and $D = {}^1/_3\mu_s'$. Recall that the diffusion approximation is applicable when $d \gg 1/z_0$ and $\mu_a \ll \mu_s'$. By substituting (7) into (1) and calculating the integral, we obtain attenuation A in the form

$$A = \frac{d}{\delta} + \ln\mu_s' - \ln\left(1 + \frac{d}{\delta}\right) + \mathrm{const} \approx \frac{d}{\delta} + \mathrm{const} = A_0 + \mu_a\left(\frac{3\mu_s'}{\mu_a}\right)^{1/2}d, \quad (8)$$

where $\delta = [3\mu_a(\mu_a + \mu_s')]^{-1/2} \approx (3\mu_a\mu_s')^{-1/2}$ is the light penetration depth in the tissue. The last equality in (8) is written in the form corresponding to the modified Lambert – Beer law (3), in which

$$\langle L\rangle_{\mathrm{int}} = \left(\frac{3\mu_s'}{\mu_a}\right)^{1/2}d. \quad (9)$$

Our aim was the experimental measurement of the reflectance of the tissue as a function of the wavelength by using optical fibres separated by a distance d (see Fig. 1). We interpreted the experimental data by using model expressions in which the diffuse reflectance or the logarithm of its reciprocal depends on the absorption coefficient μ_a of the tissue and the reduced scattering coefficient μ_s'. The value of μ_a is determined by the sum of the contributions of the chromophores present in the tissue

$$\mu_a(\lambda) = \ln 10\sum_i c_i\varepsilon_i(\lambda), \quad (10)$$

where c_i and ε_i are the chromophore molar concentrations and extinction coefficients (the extinction coefficient is the attenuation of light caused only by absorption). As chromophores we considered haemoglobin in the oxygenated and deoxygenated forms, water, fat, and exogenous PSs in some cases. The wavelength dependence of μ_s' can be described to a high degree of accuracy by a smooth power function

$$\mu_s'(\lambda) = \mu_s'(\lambda_0)\left(\frac{\lambda}{\lambda_0}\right)^{-n}, \quad (11)$$

where the exponent n for the spectral range under study (500 – 1000 nm) lies between 0.3 and 1.8 for various tissues according to experimental data [25, 26]. By substituting (10) and (11) into (8), we obtain the model dependence of the attenuation A on the wavelength and fitting parameters c_i, $\mu_s'(\lambda_0)$, n, and A_0 in the diffusion approximation. By using the method of least squares, we calculate the values of these parameters to obtain the minimal difference between the experimental and model curves. The most interesting parameters for our analysis are the concentrations c_{HbO_2} and c_{Hb} of oxy- and deoxyhaemoglobin, the degree of haemoglobin oxygenation

$$S_{O_2} = \frac{c_{HbO_2}}{c_{HbO_2} + c_{Hb}}, \quad (12)$$

and the possibility of estimating the concentration of exogenous PSs in the tissue. We will show below that the PS absorption spectrum in biological tissues is transformed in some cases. In this case, BDR spectroscopy can give only qualitative estimates of the microscopic surrounding of PSs and the nature of interaction of PSs with biological tissues. The qualitative estimate of absorption in tissues in the simulation of the BDR spectrum can be obtained by using modified Lambert – Beer law (3), in which the quantity $\langle L \rangle$ is independent of the wavelength and is a fitting parameter, while the quantity A_0 is described by a linear function of the wavelength: $A_0 = \text{const} + A_1\lambda$, where the constant and linear coefficient A_1 are also fitting parameters.

3. Results and discussion

Figure 2 shows the diffuse reflection spectra for a tumour of an experimental animal before the injection of the PS, 2 h after the injection of the PS (immediately before the exposure to laser radiation), and immediately after irradiation of the tumour by a laser. These and subsequent experiments were performed on F1 mice with Ehrlich's carcinoma intramuscularly implanted in the region of the right hind leg from the vivarium of the Cancer Research Centre, Russian Academy of Medical Sciences. Hair in the region of tumour was removed with the help of a special epilation cream Opilca. Photosense produced at the NIOPIK State Research Center was used as a PS. This PS is the optimal mixture of aluminium phthalocyanine fractions with different degrees of sulphonation. Figure 2 clearly demonstrates the potentialities of BDR spectroscopy as applied to PDT. For example, comparing the spectra recorded before and after injection of a PS, we observe the appearance of a new peak at 675 nm, which is caused by the PS contribution to absorption. Therefore, we can control the dynamics of PS concentration in various tissues *in vivo*. By comparing the spectra recorded before and after irradiation, we observe noticeable changes in the haemoglobin absorption band (500 – 600 nm), which are associated with its transition from the oxygenated to deoxygenated form due to PDT. On the one hand, this is due to enhanced utilisation of oxygen in photochemical reactions and, on the other hand, by the destruction of capillaries due to PDT. Finally, we see that PS absorption decreases after laser irradiation; this phenomenon is known

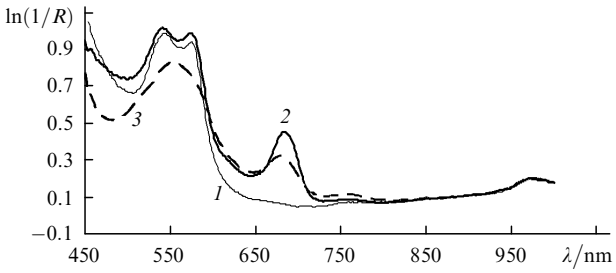

Figure 2. BDR spectra of a tumour of a mouse before the injection of Photosense (*1*), 2 hours after the injection (a dose of 4 mg kg^{-1}) (*2*), and immediately after irradiation by a laser at a wavelength of 675 nm with a dose of 30 J cm^{-2} for a power density of 100 mW cm^{-2} (*3*).

as photobleaching and makes it possible to monitor the transformation of PS itself in the course of photochemical reactions.

Note that the spectra presented in Fig. 2 were recorded when the distance d between the receiving and transmitting fibres was set equal to 3 mm, which allowed us to obtain the spectrum in a broad wavelength range from 450 to 1000 nm. For investigations in the visible range (400 – 600 nm), the spacing between the fibres varied from 2 to 4 mm. However, the probe depth turns out to be shorter than a millimetre for such a small spacing between the fibres [27]. As d is increased, the intensity of diffusely reflected light in a wavelength range of 400 – 600 nm drastically decreases due to strong absorption by haemoglobin, and the signal in this region becomes comparable to noise. An increase in the distance between the fibres increases the probe depth and makes it possible to detect more precisely small changes in the tissue absorption in the near IR range (650 – 1000 nm) due to an increase in the photon path. When only the near-IR range is investigated, the distance between the fibres is 4 – 8 mm, as a rule. If distance d is increased further (which makes it possible to increase the probe depth), the power of light incident on the tissue should be substantially increased (up to 100 mW), which was not done in our study.

Monitoring of haemoglobin oxygenation in tissues during PDT was considered in detail in [23, 27]. It was shown that the visible spectral range (500 – 600 nm) is suitable for determining the degree of oxygenation, while modified Lambert – Beer law (3) can be used for quantitative analysis. In this study, we concentrated out attention on the application of BDR spectroscopy for monitoring exogenous PSs in PDT. Figure 3 shows the BDR spectra of the tumour and normal tissue of a mouse (hip muscle of the left leg) 10 minutes after intravenous injection of Photosense (a dose of 4 mg kg^{-1}); the spectrum of the normal tissue before the injection of Photosense is also shown. Note that the Photosense absorption peak in the tumour is shifted by 7 nm to the red relative to the absorption peak in the normal tissue. This is related to a different biochemical composition of the tumour and primarily to its pH. The shift of the absorption peak is also important for the choice of the optimal laser radiation wavelength for PDT since it should correspond to the maximum of PS absorption in the tissues rather than in the model solution. Note that the absorption peak intensity in the tumour is higher than in the normal tissue, although filling of the given tumour with blood is much higher than in the normal tissue. The latter quantity can be estimated by comparing the haemoglobin absorption bandwidths (500 – 600 nm) in the tumour and in

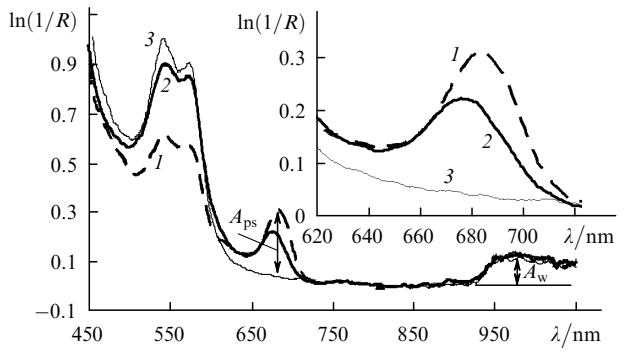

Figure 3. BDR spectra of a tumour (*1*) and a normal tissue (*2*) of a mouse 10 minutes after intravenous injection of Photosense (a dose of 4 mg kg^{-1}) and the spectrum of the normal tissue before the PS injection (*3*). The inset shows the shift of the PS absorption peak relative to the absorption peak for the normal tissue.

the normal tissue. Thus, the selectivity of Photosense accumulation in the tumour is already observed 10 minutes after its injection.

By measuring the intensity of the absorption peak in the tumour and in the normal tissue after various time intervals following the injection, we can estimate the dynamics and contrast of PS accumulation *in vivo*. Because the absorption peak in the tumour is substantially shifted and, probably, the line profile is modified, the attempts at interpreting the general diffuse reflection spectrum on the basis of the standard PS spectrum with the help of the above model are 'illegitimate'. A correct approximate estimate of the absolute PS concentration in tissues can be obtained from the ratio of absorption associated with PS and absorption of water at 975 nm [28]. This ratio can be obtained from (3) for the contribution A_{ps} of PS absorption and contribution A_w of water absorption (Fig. 3). If we assume that the mean photon paths $\langle L\rangle$ at the PS absorption wavelength (675 nm) and at the wavelength corresponding to the maximum absorption of water (975 nm) coincide, the PS concentration in the tissue is given by

$$C_{ps} = \frac{OD_w C_w}{\varepsilon_{ps}} \frac{A_{ps}}{A_w}, \tag{13}$$

where OD_w is the optical density of water ($OD_w = 0.22$ cm^{-1} at 975 nm), C_w is the relative concentration of water in the tissue (which lies between 0.6 and 0.9 for most tissues), and ε_{ps} is the PS molar extinction coefficient. In the case depicted in Fig. 3, the ratio $A_{ps}/A_w \approx 2.3$. Assuming that $C_w = 0.8$ in the tumour and considering that $\varepsilon_{ps} = 2.5 \times 10^5$ M^{-1} cm^{-1} for Photosense, we find from (13) that the PS concentration in the tumour is 1.6 μM or 1.3 mg kg^{-1}.

The dynamics of Photosense concentration in the tumour and in the normal tissue of the mouse, which is determined from the BDR spectra, is presented in Fig. 4. These results were obtained by averaging the data for three mice used in experiments; the spread in the values obtained on different animals and in different regions on the same mouse was less than 10 %. It should be recalled that, in using this approach, we assumed that the concentration of water in various tissues is constant and equal to a certain fixed value. Thus, the error in determining the PS concentration is equal to the error in the chosen value of water concentration in tissues, which may reach 30 %. In addition, we assumed that the value of $\langle L\rangle$ obtained at $\lambda = 675$ and 975 nm coincide. However, this is not true since the mean photon path in the tissue is determined by the absorption and scattering coefficients, which are functions of the wavelength. Using expression (9) derived in the diffusion approximation for the mean path length and expression (11) for estimating dependence $\mu_s'(\lambda)$, we obtain the following ratio of the photon paths at different wavelengths, which is determined by the variation of the scattering coefficient:

$$\frac{\langle L_w\rangle}{\langle L_{ps}\rangle} = \left(\frac{\lambda_{ps}}{\lambda_w}\right)^{n/2}. \tag{14}$$

Assuming in our estimate that $n \approx 1$, we find from (14) that $\langle L_w\rangle\langle L_{ps}\rangle^{-1} = (675/975)^{1/2} = 0.83$. Thus, due to the spectral dependence of the scattering coefficient, the photon path at the PS absorption wavelength is 17 % longer than at the water absorption wavelength, which results in the overstating of the PS concentration by 17 % from (13). This can be accounted for by introducing the correcting factor (14) into the right-hand side of Eqn (13).

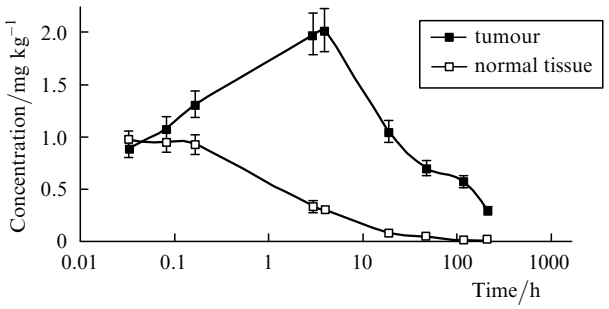

Figure 4. Dynamics of Photosense concentration after systematic injections (in a dose of 4 mg kg^{-1}) in the tumour and in the normal tissue of a mouse according to the results on diffuse reflection spectra.

Relation (13) also becomes invalid for high PS concentrations in the tissue, when the PS contribution to absorption considerably exceeds the contribution of water to absorption. Indeed, it was noted above that the modified Lambert–Beer law in differential form (6), which leads to expression (13), is only valid for small variations in the absorption coefficient. As the absorption coefficient increases, the mean photon path defined by expression (4) decreases because trajectories with short paths make a larger contribution to $\langle L\rangle$. This effect leads to smoothing of absorption peaks. In this case, deviation from linear dependence (13) of C_{ps} on A_{ps} is observed.

The application of diffusion approximation (8) for describing the relation between these quantities leads to the expression in which the contribution to absorption at high PS concentration is approximately described by the root dependence on the concentration:

$$A_{ps} = \left(3\mu_s'\right)^{1/2} d\left[\left(\mu_a^0 + \ln 10\varepsilon_{ps}C_{ps}\right)^{1/2} - \left(\mu_a^0\right)^{1/2}\right]. \tag{15}$$

To verify this effect, we performed an experiment with model samples containing intralipid, whole blood, and PS. Intralipid consists of water, lipid, and a stabiliser and is used in medicine for intravenous injections. In biophotonics, it is

used as a phantom for simulating the scattering properties of tissues. Since intralipid was diluted to the required concentration with the help of saline (physiological solution), we can assume that the addition of erythrocyte mass or whole blood does not lead to hemolysis or substantial aggregation of erythrocytes. The initial solution contained 1.6 % intralipid and 1 % whole blood for simulating the scattering and absorbing properties of the tissue (which, according to our estimates is characterised by values of $\mu_s' = 15 \pm 5\ \mathrm{cm}^{-1}$ and $\mu_a = 0.04\ \mathrm{cm}^{-1}$). The scattering coefficient was calculated using the data obtained in [29]. If a more exact value of the scattering coefficient of the intralipid solution is required, independent measurements should be performed (e.g., it is necessary to measure the displacement of the intensity peak in the case of oblique incidence). However, this was not required in our experiment; it was only important that the value of scattering coefficient was within its range of variation in the tissues. The absorption coefficient was determined assuming that predominant contribution to absorption comes from haemoglobin with a degree of oxygenation of 75 % at a wavelength of 675 nm.

Then we added Photosense to this solution and measured diffuse reflection spectra for various concentrations of this agent in a range of 0 – 2 mg L^{-1}. The transmitting and receiving optical fibres were spaced at a distance of 8 mm from each other in contact with the surface of the solution. The obtained spectra are shown in Fig. 5. The sharp increase in attenuation on the side of short wavelengths is due to absorption by haemoglobin, while the peak at 975 nm is due to absorption by water. The contribution of PS absorption at a wavelength of 675 nm can easily be separated against the smooth background of solution absorption. The dependence of the contribution of PS absorption on the PS concentration, which was obtained from the diffuse reflection spectra, is presented in Fig. 6. As expected, the $A_{ps}(C_{ps})$ dependence deviated from linearity for high concentrations. The same figure shows the theoretical curve corresponding to diffusion approximation (15). The values of μ_a^0 and μ_s' were chosen so that the difference in the standard deviations between the theoretical curve and experimental data was minimal. One can see from Fig. 6 that diffusion approximation successfully describes the effect of smoothing of the absorption peaks.

The experimental dependence of A_{ps} on C_{ps} depicted in Fig. 6 can subsequently be used for calibration to determinie the absolute PS concentration in tissues. We will call this method the standard sample method. Similar curves were

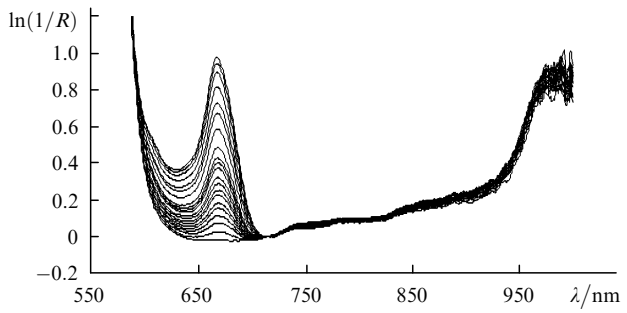

Figure 5. BDR spectra of solutions of intralipid (1.5 %), blood (1 %), and Photosense in an interval of 0 – 2 mg L^{-1}. The interval between the first 12 spectra is 0.04 mg L^{-1} and subsequent intervals are 0.2 mg L^{-1}.

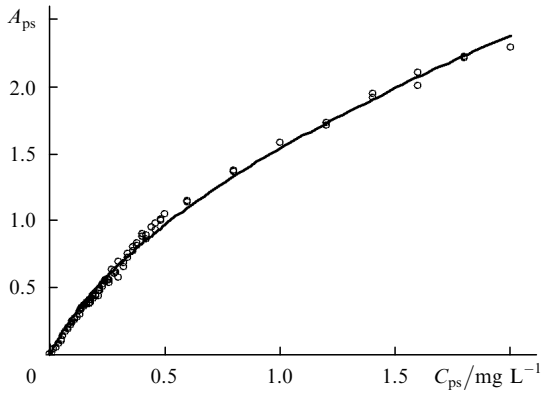

Figure 6. Contribution to absorption of Photosense (A_{ps}) in the solution of intralipid (1.6 %) and blood (1 %) as a function of its concentration.

also plotted in our earlier studies for other concentrations of intralipid (1.2 % – 2.2 %) and blood (0 % – 5 %) in a model solution to estimate the effect of variations of the scattering and absorption coefficients of the tissue on the accuracy of determining the PS concentration in tissues with the help of the standard sample method. The deviations in the results upon variation of the absorption and scattering coefficients over such wide ranges did not exceed 50 %. Thus, if the PS concentrations in tissues are so low that the contribution of PS absorption is smaller than the contribution of absorption by water at $\lambda = 975$ nm, expression (13) can be used for estimating the PS concentration. If the PS contribution exceeds the contribution due to water absorption, the effect of smoothing of absorption should be taken into account and the standard sample method should be employed. Naturally, the latter method successfully operates for low concentrations as well; in this case, the PS concentration can be estimated independently of the water absorption contribution. It should also be noted that the method of standard samples does not take into account possible variations in the PS extinction coefficient upon PS binding with biomolecules in tissues. This circumstance can be partly taken into account by using blood plasma (which is closer to tissues in its properties) instead of physiological saline solution for preparing standard samples.

Concluding the section, we present some results which make it possible to observe qualitative changes in tissues from the PS absorption spectra in these tissues. Figure 7 shows the absorption spectra of a tumour of a mouse after intravenous injection of Teraphthal in a dose of 20 mg kg^{-1}. This preparation (cobalt phthalocyanine) is being developed at the NIOPIK State Research Center for dark therapy of tumour in combination with ascorbic acid. The shape of the spectrum recorded 10 minutes after the injection corresponds to the Teraphthal absorption spectrum in the solution (except a slight shift of the absorption peak to the IR range). However, two days later, the absorption peak of the tumour becomes noticeably broader due to the formation of aggregates and nanoparticles of Teraphthal molecules in a more acidic medium of the tumour. Probably, the balance of calcium ions also plays an important role in aggregation since the calcium salt of Teraphthal is insoluble in water. This result is interesting since Teraphthal nanoparticles together with ultrasound or pulsed laser radiation may lead to destruction of tumours. Diffuse reflection spectroscopy is the only method of *in vivo* monitoring of

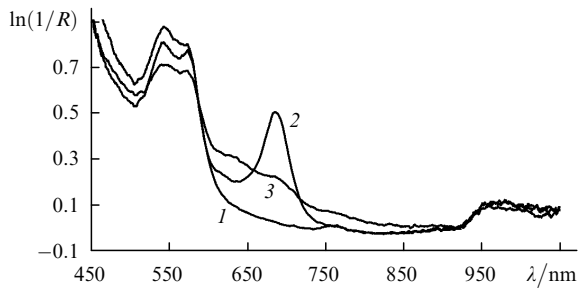

Figure 7. BDR spectra of the tumour before (*1*) and 10 min (*2*), and 2 days (*3*) after the injection of Teraphthal (in a dose of 20 mg kg^{-1}).

the formation of nanoparticles in tissues since this substance does not fluoresce.

The latter results concerns indocyanin green, which is widely used in medicine as a PS and is characterised by a high-intensity absorption peak in the near IR region (800 nm). It was reported in recent publications [30] that this PS is effective in phototherapy of tumours. Most likely, the therapeutic effect is ensured by the combination of the thermal and photochemical action. For this reason, the results on the absorption spectra in tissues are of considerable importance. The BDT spectroscopic data on accumulation of indocyanin green in skin as a result of application are available in the literature [31], but the results on selectivity of accumulation in tumours after intravenous injection are absent to our knowledge.

Figure 8 shows the diffuse reflection spectra of a tumour and a normal tissue of a mouse 90 minutes after intravenous injection of indocyanin green (in a dose of 40 mg kg^{-1}). In spite of the short time elapsed after the injection, the curves corresponding to the tumour and to the normal tissue differ substantially. Because the dependence of the PS concentration on the PS contribution to absorption is approximately described by a quadratic function, the ratio of PS concentrations is equal to nine for the ratio of absorptions in the tumour and in the normal tissue equal to three at $\lambda = 770$ nm. No transformation of the absorption spectrum in the tissue was observed as compared to the spectrum of absorption of this dye in blood plasma. However, the exposure of a tissue to laser radiation with $\lambda = 805$ nm leads to intense bleaching of this PS and its conversion into a colourless form. This effect may play a positive role in phototherapy since light irradiating a tissue is strongly screened by its upper layers due to such a large

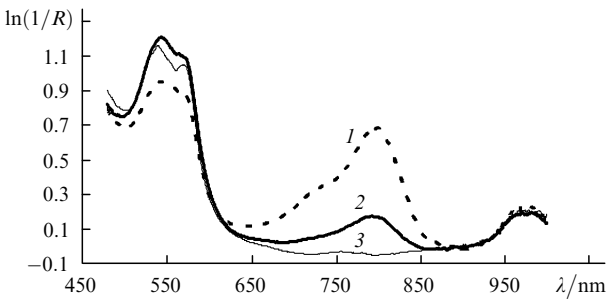

Figure 8. BDR spectra of a tumour (*1*) and a normal tissue (*2*) of a mouse 90 minutes after the injection of indocyanin green (in a dose of 40 mg kg^{-1}) and the spectrum of the normal tissue prior to the injection of the dye (*3*).

contribution to dye absorption. In the course of irradiation, the dye is burnt out and, hence, the light penetration depth in the tissue increases. There is no risk of overdose in irradiation of normal tissues since selectivity of action in this case is determined primarily by the selectivity of dye accumulation.

4. Conclusions

The results described in the paper demonstrate the efficient application of diffuse reflection spectroscopy for monitoring the state of tissues in PDT. The simple experimental technique for detecting BDR spectra of tissues under stationary conditions with the help of a fibre-optic probe with a fixed distance between the transmitting and receiving fibres ensures the required accuracy of monitoring the degree of haemoglobin oxygenation in tissues during PDT and makes it possible to estimate the dynamics of PS concentration in tumours and normal tissues after intravenous injection, as well as PS photodestruction during laser irradiation of a tumour in PDT. In some cases, this method makes it possible to determine the type of PS localisation in tissues at subcellular level, as well as PS aggregation (or, conversely, monomerisation) in the case of PS binding with biomolecules. This information is valuable for the choice of dyes used as effective PSs for PDT and photothermolysis; it can also be used for the development of optimal policy in PDT (PS injection dose, time interval between PS injection and irradiation, irradiation doses and power density in laser irradiation).

Acknowledgements. This work was supported by the Russian Foundation for Basic Research (Grant No. 06-02-17468) and the Research Program 'Development and Mastering of New Methods of Health Protection and Methods of Prophylactics, Diagnostics, and Treatment of Oncological, Infectious, and Other Dangerous Disease' (2003 – 2006).

References

1. Jöbsis F.F. *Science*, **198**, 1264 (1977).
2. Mourant J.R., Bigio I.J., in *Biomedical Photonics Handbook*. Ed. by Tuan Vo-Dinh (Boca Raton, USA: CRC Press, 2003).
3. Wallace V.P., Crawford D.C., Mortimer P.S., Ott R.J., Bamber J.C. *Phys. Med. Biol.*, **45**, 735 (2000).
4. Koenig F., Larne R., Enquist H., McGovern F.J., Schomacker K.T., Kollias N., Deutsch T.F. *Urology*, **51**, 342 (1998).
5. Zonios G., Perelman L.T., Backman V., Manoharan R., Fitzmaurice M., Van Dam J., Feld M.S. *Appl. Opt.*, **38**, 6628 (1999).
6. Mourant J.R., Bigio I.J., Boyer J., Johnson T.M., Lacey J. *Biomed. Opt.*, **1**, 1 (1996).
7. Utzinger U., Brewer M., Silvio E., Gershenson D., Blast R.C., Follen M., Richards-Kortum R. *Lasers Surg. Med.*, **28**, 56 (2001).
8. Stratonnikov A.A., Edinac N.E., Klimov D.V., Linkov K.G., Loschenov V.B., Luckjanets E.A., Meerovich G.A., Vakulovskaya E.G. *Proc. SPIE Int. Soc. Opt. Eng.*, **2924**, 49 (1996).
9. Weersink R.A., Hayward J.E., Diamond K.R., Patterson M.S. *Proc. SPIE Int. Soc. Opt. Eng.*, **2972**, 136 (1997).
10. Ballangrud A.M., Barajas O., Brown K., Miller G.G., Moore R.B., Tulip J. *Lasers Med. Sci.*, **12**, 237 (1997).
11. Cubeddu R., Canti G., D'Andrea C., Pifferi A., Taroni P., Torricelli A., Valentini G. *J. Photochem. Photobiol. B*, **60**, 73 (2001).

12. Weersink R.A., Wilson B.C., Patterson M.S. *Proc. SPIE Int. Soc. Opt. Eng.*, **4613**, 135 (2002).
13. Solonenko M., Cheung R., Busch T.M., Kachur A., Vulcan T., Zhu T.C., Wang H.W., Hahn S.M., Yodh A.G. *Phys. Med. Biol.*, **47**, 857 (2002).
14. Stratonnikov A.A., Ermishova N.V., Meerovich G.A., Kudashev B.V., Vakulovskaya E.G., Loschenov V.B. *Proc. SPIE Int. Soc. Opt. Eng.*, **4613**, 162 (2002).
15. Mourant J.R., Johnson T.M., Los G., Bigio I.J. *Phys. Med. Biol.*, **44**, 1397 (1999).
16. Patterson M.S., Chance B., Wilson B.C. *Appl. Opt.*, **28**, 2331 (1989).
17. Doornbos R.M.P., Lang R., Aalders M.C., Cross F.W., Sterenborg H.J. *Phys. Med. Biol.*, **44**, 967 (1999).
18. Meglinski I.V., Matcher S.J. *Physiol. Meas.*, **23**, 741 (2002).
19. Duysens L.N.M. *Biochim. Biophys. Acta*, **19**, 1 (1956).
20. Talsma A., Chance B., Graaf R. *J. Opt. Soc. Am. A*, **18**, 932 (2001).
21. Finlay J.C., Foster T.H. *Opt. Lett.*, **29**, 965 (2004).
22. Sassaroli A., Fantini S. *Phys. Med. Biol.*, **49**, 255 (2004).
23. Stratonnikov A.A., Loschenov V.B. *J. Biomed. Opt.*, **6**, 457 (2001).
24. Kienle A., Patterson M.S. *J. Opt. Soc. Am.*, **14**, 246 (1997).
25. Torricelli A., Pifferi A., Taroni P., Giambattistelli E., Cubeddu R. *Phys. Med. Biol.*, **46**, 2227 (2001).
26. Bashkatov A.N., Genina E.A., Kochubey V.I., Tuchin V.V. *J. Phys. D: Appl. Phys.*, **38**, 2543 (2005).
27. Stratonnikov A.A., Ermishova N.V., Loshchenov V.B. *Kvantovaya Elektron.*, **32**, 917 (2002) [*Quantum Electron.*, **32**, 917 (2002)].
28. Matcher S.J., Cope M., Delpy D.T. *Proc. SPIE Int. Soc. Opt. Eng.*, **1888**, 239 (1993).
29. Jacques S.L. http://omlc.ogi.edu/spectra/intralipid/index.html.
30. Urbanska K., Romanowska-Dixon B., Matuszak Z., Oszajca J., Nowak-Sliwinska P., Stochel G. *Acta Biochim. Polonica*, **49**, 387 (2002).
31. Genina E.A., Bashkatov A.N., Kochubei V.I., Tuchin V.V., Altshuler G.B. *Pis'ma Zh. Tekh. Fiz.*, **27**, 63 (2001).